Available online at www.sciencedirect.com

ScienceDirect

JOURNAL OF IRON AND STEEL RESEARCH, INTERNATIONAL. 2015, 22(10): 954-960

Multi-objective Optimization of Continuous Drive Friction Welding Process Parameters Using Response Surface Methodology with Intelligent Optimization Algorithm

P. M. AJITH[1], T. M. AFSAL HUSAIN[1], P. SATHIYA[1], S. ARAVINDAN[2]

(1. Department of Production Engineering, National Institute of Technology, Tiruchirappalli 620015, Tamilnadu, India;
2. Department of Mechanical Engineering, Indian Institute of Technology Delhi, New Delhi 110016, India)

Abstract: The optimum friction welding (FW) parameters of duplex stainless steel (DSS) UNS S32205 joint was determined. The experiment was carried out as the central composite array of 30 experiments. The selected input parameters were friction pressure (F), upset pressure (U), speed (S) and burn-off length (B), and responses were hardness and ultimate tensile strength. To achieve the quality of the welded joint, the ultimate tensile strength and hardness were maximized, and response surface methodology (RSM) was applied to create separate regression equations of tensile strength and hardness. Intelligent optimization technique such as genetic algorithm was used to predict the Pareto optimal solutions. Depending upon the application, preferred suitable welding parameters were selected. It was inferred that the changing hardness and tensile strength of the friction welded joint influenced the upset pressure, friction pressure and speed of rotation.

Key words: friction welding; response surface methodology; genetic algorithm; Pareto front; multi-objective optimization; duplex stainless steel

The basic microstructure of the duplex stainless steel (DSS) consists of 50:50 ratios of ferrite (α) and austenite (γ) phases. Major applications are in the fields of petrochemical, chemical manufacturing, oil and gas pipeline industries. The above industries use DSS because of its higher strength and higher corrosion resistance. Compared with austenitic stainless steel, it is made of more ferromagnetic substances with a high thermal conductivity and a lower thermal expansion. Some of the other mechanical properties found from the literature are its excellent toughness and high fatigue strength at lower temperatures, sufficient formality and weldability and exceptional resistance to stress corrosion cracking, pitting and general corrosion[1-3].

Some of the disadvantages in the application of the duplex stainless steels at 250–1 000 °C are the formation of various intermetallic phases, precipitates and other phases[4-6]. The complex problems are due to the long time operation above 250 °C. In the temperature range of 250–500 °C, the α'-formation happens in the ferritic phase. Thus, the problems facing DSS are subsequent loss of toughness and ferrite hardening[7-9]. The good quality of the friction welded joint produced depends upon the proper selection and accurate setting of parameters[10]. Finding the optimum process parameters and selecting the proper combinations of input parameters by conducting so many trial and error experiments remain costly and are a time consuming process[11]. Use of response surface methodology (RSM)[12] can prevent this problem and create models which can sufficiently forecast the relation between input parameters and the output. Paventhan et al.[13] investigated the effect of the friction welding (FW) parameters of AISI 1040 grade medium carbon steel and AISI 304 austenitic stainless steel joint. The selected input parameters for the study were friction pressure, forging pressure, friction time and forging time, which had a considerable impact on strength of the joints. The parameters were optimized by using RSM to obtain maximum strength. Ahmet et al.[14] conducted friction welding of dissimilar materials like Cu and Fe. They studied friction welded joint interface mechanical and metallurgical characteristics. They set the different ranges of the parameters and carried out the experiment. The experimental results were analyzed for the effect of the parameters on mechanical properties of the welded joint. The responses taken for this study were hardness (H), tensile strength (TS) and yield strength (YS). Sathiya et al.[15] studied the effect of welding parameters by artificial neural network (ANN) technique. The study concentrated on minimizing metal loss during the FW and the quality of the stainless steel (AISI 304) joint. Using ANN, optimized results were obtained and the optimized values were in agreement with the experimental results. Ananthapadmanaban et al.[16] studied the experimental values of the friction

Biography: P. M. AJITH, Doctor; **E-mail:** psathiya@nitt.edu; **Received Date:** June 26, 2014

welded mild steel joints interface. Hardness variations at different welding zones were measured and compared. Sahin[17] studied the process austenitic stainless steels materials by friction welding processes. A comparative study determined the welded joint tension, fatigue, hardness and impact tests. Gunaraj and Murugan[18] optimized the submerged arc welding (SAW) processes using RSM. The model developed the simultaneous regression equations. Input parameters selected were open circuit voltage (OCV), wire feed rate (WFR), speed of welding (S), and nozzle-to-plate distance. The outputs considered were penetration, reinforcement, width and percentage dilution. The study concluded that increasing S decreases the output of the welded joint.

Most previous literatures studied the weld quality in terms of good mechanical properties of friction welded joint. During FW process, refining of grain size was helpful to increase the strength. Most studies concentrated on how to improve the tensile strength and hardness. The input parameter was optimized to obtain maximum quality of welded joint.

The present work to create models based on RSM in order to forecast the hardness and tensile strength as a function of vital input parameters in FW. A central composite design was used to recognize the input parameters and to compare their impact on the hardness and tensile strength and to find which one is mainly important. When two outputs are taken, the problem becomes multifaceted. Simultaneous optimization of H and TS is focused in this study. Genetic algorithm (GA) with RSM model optimization was used for maximizing the TS and H of the joints.

1 Methodology

The design of the experiment depended upon the number of input parameters and the level was fixed according to their ranges. In this investigation, the selected input parameters were friction pressure, upset pressure, speed and burn-off length. The range of the experiment was fixed and preliminary trail runs were conducted. After the friction, welding trail runs were checked to identify any defect in joint interface. During the inspection, no defects were found in the weld joint zones. Then, the input parameters were fixed. Table 1 presents the process variables and their range.

A central composite rotatable factorial design consisting of 30 number runs were selected[13]. Designed experiment runs and their predicted and observed values are presented in the Table 2.

Table 1 Process variables and its bounds

Parameter	Unit	Notation	Factor levels				
			-2	-1	0	1	2
Friction pressure	MPa	F	45	65	85	105	125
Upset pressure	MPa	U	140	155	170	185	200
Speed	r/min	S	1000	1250	1500	1750	2000
Burn-off length	mm	B	2.5	3	3.5	4	4.5

Table 2 Central composite design with observed and predicted responses

Serial No.	Coded unit				Actual value				H/MPa		Tensile strength/MPa	
	F	U	S	B	F/MPa	U/MPa	S/(r·min^{-1})	B/mm	Observed	Predicted	Observed	Predicted
1	–1	–1	–1	–1	65	155	1 250	3	285	283.93	681	686.28
2	1	–1	–1	–1	105	155	1 250	3	292	291.26	780	777.12
3	–1	1	–1	–1	65	185	1 250	3	298	297.26	802	799.45
4	1	1	–1	–1	105	185	1 250	3	305	304.59	841	847.28
5	–1	–1	1	–1	65	155	1 750	3	291	288.43	802	803.78
6	1	–1	1	–1	105	155	1 750	3	295	295.76	810	816.12
7	–1	1	1	–1	65	185	1 750	3	302	301.76	830	834.45
8	1	1	1	–1	105	185	1 750	3	309	309.09	805	803.78
9	–1	–1	–1	1	65	155	1 250	4	290	287.09	778	776.95
10	1	–1	–1	1	105	155	1 250	4	295	294.43	813	819.28
11	–1	1	–1	1	65	185	1 250	4	301	300.43	810	814.62
12	1	1	–1	1	105	185	1 250	4	312	307.76	818	813.95
13	–1	–1	1	1	65	155	1 750	4	293	291.59	816	820.45
14	1	–1	1	1	105	155	1 750	4	297	298.93	784	784.28
15	–1	1	1	1	65	185	1 750	4	306	304.93	775	775.62
16	1	1	1	1	105	185	1 750	4	315	312.26	691	696.45
17	–2	0	0	0	45	170	1 500	3.5	291	294.23	788	786.03
18	2	0	0	0	125	170	1 500	3.5	308	308.90	799	797.70
19	0	–2	0	0	85	140	1 500	3.5	300	301.23	787	779.20
20	0	2	0	0	85	200	1 500	3.5	325	327.90	809	804.53
21	0	0	–2	0	85	170	1 000	3.5	280	283.63	795	791.87
22	0	0	2	0	85	170	2 000	3.5	292	292.63	800	791.87
23	0	0	0	–2	85	170	1 500	2.5	286	284.96	804	800.20
24	0	0	0	2	85	170	1 500	4.5	289	291.29	787	783.53
25	0	0	0	0	85	170	1 500	3.5	287	288.13	794	791.87
26	0	0	0	0	85	170	1 500	3.5	290	288.13	792	791.87
27	0	0	0	0	85	170	1 500	3.5	285	288.13	788	791.87
28	0	0	0	0	85	170	1 500	3.5	289	288.13	791	791.87
29	0	0	0	0	85	170	1 500	3.5	288	288.13	790	791.87
30	0	0	0	0	85	170	1 500	3.5	287	288.13	796	791.87

The effects of the parameters were estimated by linear, quadratic and two-way interaction method.

2 Experimental

The experimental work was carried out by charge-coupled device (CCD) with full replication. A 150 kN capacity continuous FW machine was used. The material selected was DSS (UNS S32205) with dimensions of 100 mm in length and diameter of 15 mm. Table 3 presents the base material chemical composition.

Table 3 Chemical composition of base material mass%

C	Si	Mn	P	S	Cr	Mo	Ni	N	Fe
0.021	0.357	1.61	0.026	0.001	22.50	3.38	4.79	0.193	Balance

The surfaces of samples were cleaned by acetone. The selected welding parameters and their ranges were friction pressure (45 to 125 MPa), upset pressure (140 to 200 MPa), speed of rotation (1 000 to 2 000 r/min) and burn-off length (2.5 to 4.5 mm). For mechanical and metallurgical study, the flash from the surface was removed. The specimens were cut into 10 mm×10 mm. They were mounted and polished by SiC abrasive paper with different grit sizes from 180 to 1 200. By using 3 μm diamond paste, the samples were polished as per the ASTM3-11 standard. The samples were subjected to electrolytic etching by applying 10% oxalic acid at 9 V for 30 s. The tensile tests and microhardness test were used to evaluate the mechanical properties of the welded joint. For the tensile test, ASTM E8 standard was used. The average values were calculated from three measurements taken for every welding experiment. Vickers microhardness test was carried out at 4.9 N load for 10 s. The hardness was taken on a transverse section of the weld centre.

3 Development of Model

The developed model representing hardness and tensile strength is

$$Y=f(\mathrm{F, U, S, B}) \tag{1}$$

where, Y is the response or yield.

The model was created by using design expert software at a confidence level of 95%. Hardness and tensile strength were expressed as a nonlinear function of process parameters. Thus, the second degree response surface could be expressed as

$$Y=b_0+b_1\mathrm{F}+b_2\mathrm{U}+b_3\mathrm{S}+b_4\mathrm{B}+b_{12}\mathrm{FU}+b_{13}\mathrm{FS}+b_{14}\mathrm{FB}+b_{23}\mathrm{US}+b_{24}\mathrm{UB}+b_{34}\mathrm{SB}+b_{11}\mathrm{F}^2+b_{22}\mathrm{U}^2+b_{33}\mathrm{S}^2+b_{44}\mathrm{B}^2 \tag{2}$$

where, b_0 is the average of responses; and b_1, b_2 b_3, b_4, b_{11}, b_{12}, b_{13}, ..., b_{44} are the response coefficients. Design expert software Version 6.0.8 was used to calculate the coefficient values[19].

In the hardness model, the model terms S^2, B^2, FU, FS, FB, US, UB and SB were found insignificant and therefore removed. In the case of tensile strength, all square terms were found insignificant and eliminated. However, speed was not eliminated since it supported hierarchy of the model.

The final model was created using only major terms, and the developed final experimental relationship both in coded and real factors are given below.

Final equations in terms of coded factors

$$\mathrm{H}=288.13+3.67\mathrm{F}+6.67\mathrm{U}+2.25\mathrm{S}+1.58\mathrm{B}+3.36\mathrm{F}^2+6.61\mathrm{U}^2 \tag{3}$$

$$\mathrm{TS}=791.87+2.92\mathrm{F}+6.33\mathrm{U}+0\times\mathrm{S}-4.17\mathrm{B}-10.75\mathrm{FU}-19.62\mathrm{FS}-12.12\mathrm{FB}-20.62\mathrm{US}-18.87\mathrm{UB}-18.50\mathrm{SB} \tag{4}$$

Final equations in terms of actual factors

$$\mathrm{H}=1\,082.018\,99-1.244\,40\mathrm{F}-9.543\,06\mathrm{U}+9\times10^{-3}\mathrm{S}+3.166\,67\mathrm{B}+8.398\,44\times10^{-3}\mathrm{F}^2+0.029\,375\mathrm{U}^2 \tag{5}$$

$$\mathrm{TS}=4\,319.004\,86+16.368\,75\mathrm{F}+20.526\,39\mathrm{U}+1.786\,63\mathrm{S}+744.562\,50\mathrm{B}-0.035\,833\mathrm{FU}-3.925\,00\times10^{-3}\mathrm{FS}-1.212\,50\mathrm{FB}-5.5\times10^{-3}\mathrm{US}-2.516\,67\mathrm{UB}-0.148\,00\mathrm{SB} \tag{6}$$

The satisfactoriness of the developed empirical relationship was checked by ANOVA technique[20]. The results of ANOVA are shown in Table 4.

The model F-values of 106.23 and 113.29, for H and TS respectively, implied that the models were significant. The 'predicted R^2' values were in reasonable agreement with the 'adjusted R^2' values. The 'adequate precision' measured the signal to noise ratio. A ratio greater than 4 was wanted. There was a sufficient signal in both models. Therefore, these models could be used to find the way to design space. Each predicted value coordinated well with its experimental value, as shown in the relationship graph in Figs. 1 and 2.

4 Optimization

4.1 GA optimization

The GA works evenly well both in continuous or discrete search space. The flow chart of the GA is shown in Fig. 3.

The following steps were carried out in GA.

Step 1: The algorithm stopped when the number of generations reached the value of generations.

Step 2: The algorithm stopped after running for an amount of time in seconds equal to the time limit.

Step 3: The algorithm stopped when the value of the fitness function for the best point in the current population was less than or equal to the fitness limit.

Step 4: The algorithm stopped when the weighted average changed in the fitness function value over Stall generations and was less than function tolerance.

Table 4 ANOVA results for hardness and tensile strength

		Hardness		Tensile strength	
		F-value	Prob > *F*-value	*F*-value	Prob > *F*-value
Source	Model	106.232	< 0.000 1	113.287	< 0.000 1
	F	68.281 4	< 0.000 1	7.727 94	0.011 9
	U	225.724	< 0.000 1	36.438	< 0.000 1
	S	25.711 3	< 0.000 1	0	1.000 0
	B	12.732 2	0.001 6	15.7713	0.000 8
	F2	67.930 2	< 0.000 1		
	U2	262.946	< 0.0001		
	FU			69.986 7	< 0.000 1
	FS			233.248	< 0.000 1
	FB			89.0353	< 0.000 1
	US			257.624	< 0.000 1
	UB			215.761	< 0.000 1
	SB			207.273	< 0.000 1
Model statistics	R^2	0.97		0.98	
	Adjusted R^2	0.96		0.97	
	Predicted R^2	0.92		0.94	
	Adequate precision	42.16		51.73	

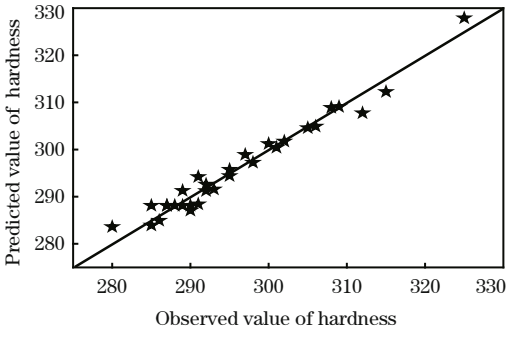

Fig. 1 Correlation graph for hardness

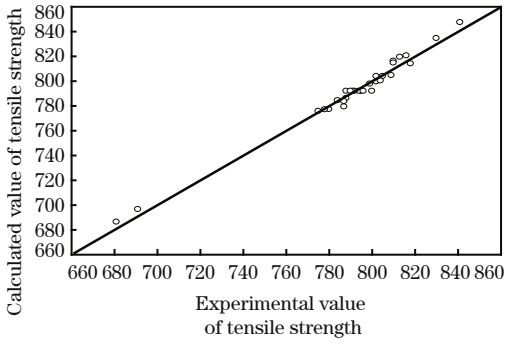

Fig. 2 Correlation graph for tensile strength

Step 5: The algorithm stopped if there was no improvement in the objective function during an interval of time in seconds equal to Stall time limit.

Step 6: The algorithm ran until the weighted average changed in the fitness function value over Stall generations and was less than function tolerance.

Step 7: The nonlinear constraint tolerance was not used as a stopping criterion. It was used to determine the feasibility with respect to nonlinear constraints.

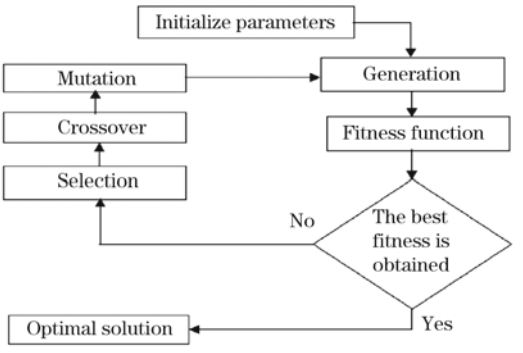

Fig. 3 Flow chart of GA for optimization

This investigation aims to study the influence of FW parameters, and to set up a relation between input and responses. ANOVA was used to analyze the significant factors.

4.2 Optimization procedure

Pareto optimal solutions were generated by MATLAB (R2010a) tool box for H and TS using 'gamultiobj' function. The MATLAB function 'gamultiobj' used a controlled elitist GA with better fitness value (rank)[21]. The developed RSM model was used to write the MATLAB function. The H and TS to be maximized was negated in the fitness function since 'gamultiobj' minimized all the objectives. The limit ranges for RSM design for the input variables are given below:

limits on friction pressure 65 MPa≤ F ≤ 105 MPa
limits on upset pressure 155 MPa≤ U ≤ 185 MPa
limits on speed 1250 r/min≤ S ≤ 1750 r/min
limits on burn-off length 3 mm≤ B ≤ 4 mm.

The following GA algorithm options were set and listed in Table 5.

Table 5 Genetic algorithm settings

Population type	Double vector
Population size	70
Creation function	Feasible population
Selection function	Tournament of size two
Crossover fraction	0.75
Crossover function	Scattered
Mutation function	Adaptive feasible
Direction for migration	Forward
Migration fraction	0.2
Distance measure function	Distance crowding
Pareto front population fraction	0.35

The average weighted change in the fitness function value above 100 generations was used as the norm for terminating the algorithm. The optimized Pareto front achievement after 315 iterations is shown in Fig. 4.

The input decision variables corresponding to each of the Pareto optimal solutions are tabulated in Table 6.

From Table 6, the decision variables were taken to obtain localized optimal operating conditions for H and TS.

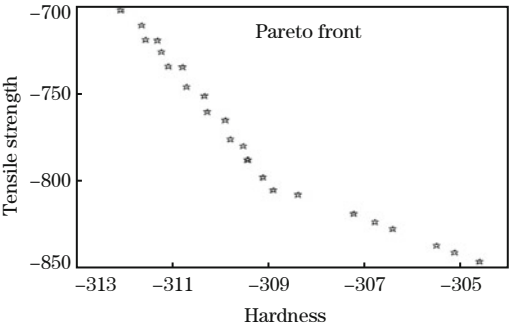

Fig. 4 Pareto optimal set of solutions

Table 6 Process decision variables corresponding to each of the Pareto optimal solutions

Serial No.	Friction pressure/ MPa	Upset pressure/ MPa	Speed/ ($r \cdot min^{-1}$)	Burn-off length/ mm	Hardness/ HV	Tensile strength/ MPa
1	105.00	185.00	1 727.37	4.00	312.06	701.78
2	105.00	184.92	1 697.31	3.98	311.63	710.62
3	105.00	185.00	1 727.37	3.83	311.53	718.96
4	105.00	184.81	1 727.37	3.83	311.28	719.41
5	104.99	184.98	1 697.28	3.83	311.21	726.22
6	105.00	185.00	1 727.37	3.69	311.07	734.30
7	105.00	184.79	1 727.37	3.69	310.78	734.92
8	105.00	185.00	1 727.37	3.57	310.69	746.40
9	105.00	184.92	1 697.31	3.57	310.32	751.68
10	105.00	185.00	1 727.37	3.43	310.26	760.86
11	105.00	184.92	1 697.31	3.43	309.87	765.60
12	105.00	185.00	1 727.36	3.28	309.78	776.61
13	105.00	185.00	1 697.31	3.28	309.50	780.48
14	104.99	185.00	1 727.36	3.17	309.42	788.24
15	105.00	185.00	1 727.37	3.17	309.41	788.43
16	105.00	184.99	1 727.36	3.07	309.10	798.37
17	105.00	185.00	1 727.37	3.00	308.89	805.76
18	104.49	185.00	1 697.31	3.00	308.36	808.67
19	105.00	184.98	1 250.01	3.83	307.20	819.56
20	105.00	185.00	1 250.01	3.69	306.77	824.38
21	105.00	185.00	1 250.01	3.57	306.40	828.26
22	105.00	185.00	1 250.01	3.28	305.48	837.98
23	104.99	185.00	1 250.01	3.17	305.11	841.72
24	105.00	185.00	1 250.00	3.00	304.59	847.29
25	105.00	185.00	1 250.00	3.00	304.59	847.29

5 Results and Discussion

Mechanical properties of friction welded joints were predicted from RSM model. The responses were Hand TS. Friction pressure, upset pressure, speed and burn-off length were chosen as process input parameters. The developed RSM model correlated with experimental results with R^2=0.97 for hardness and R^2 = 0.98 for tensile strength. From Table 4, it is clear that the highest F-values were obtained in friction pressure. Thus, significance was on tensile strength followed by upset pressure and speed. In the case of hardness, friction pressure had high significance followed by upset pressure and speed. It is concluded that the required quality of the friction welded joint agreed with the Pareto optimal solutions set to select the hardness and tensile values. The analysis of both tensile strength and hardness model and experimental values were found almost closer. The conformation results are presented in Table 7.

Table 7 Confirmation test results

Serial No.	F/ MPa	B/ mm	U/ MPa	S/ (r·min^{-1})	Hardness/HV		Tensile strength/MPa	
					Predicted	Observed	Predicted	Observed
1	105	3.25	185	1 250	305.48	310	837.98	840
2	105	3.5	185	1 250	306.40	302	828.26	830
3	105	3.0	185	1 700	308.36	305	808.67	812

The individual parameter to response effects was analyzed using the developed RSM model. Figs. 5, 6, 7, and 8 present the individual performance of the output with actual friction welding parameters.

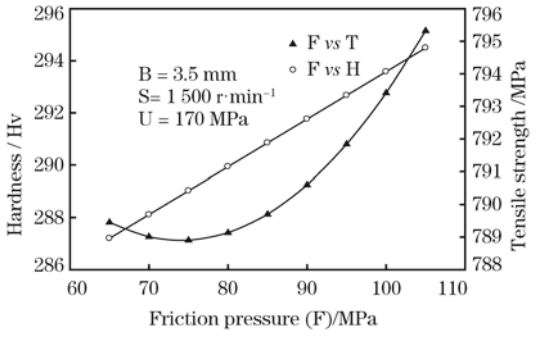

Fig. 5 Effect of friction pressure on hardness and tensile

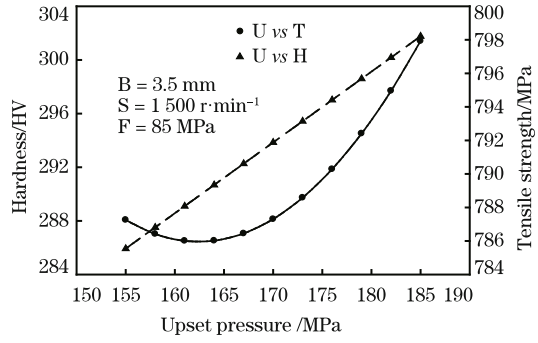

Fig. 6 Effect of upset pressure on hardness and tensile strength

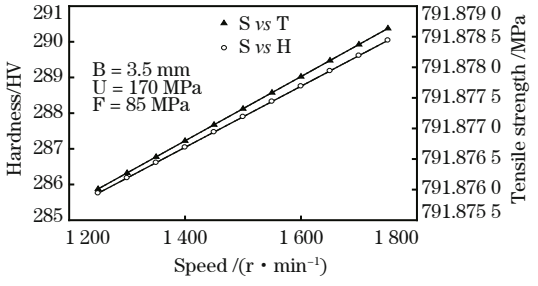

Fig. 7 Effect of speed on hardness and tensile strength

Fig. 5 shows the effect of friction pressure on hardness and tensile strength. Friction pressure varied from 45 to 125 MPa while the remaining parameters namely upset pressure, rotational speed and burn-off length were kept at 170 MPa, 1 500 r/min, and 3.5 mm, respectively. Effect of increasing friction pressure was an increase in hardness and tensile strength. Because of higher friction pressure, more heat was generated. During the upsetting time, more plastic stage material was formed as flashes and less plastic stage material was retained in the weld zone and fine grains were also formed in the weld and HAZ region. Fukumoto et al.[22] investigated friction welding parameters and stated that the higher the forging pressure, the more grain refinement took place and lower forging pressure produced lesser refinement. It was also revealed that the middle area consisted of fine grains, while the tangential area had coarse grains. The dynamic recrystallization caused finer grains on the middle area. The temperature of the tangential area would be higher.

Fig. 6 presents the effect of upset pressure on hardness and tensile strength. It shows that the upset pressure varied from 145 to 200 MPa while the friction pressure, rotational speed and burn-off length were kept at 85 MPa, 1 500 r/min, and 3.5 mm, respectively. The Effect of increasing upset pressure was that H and TS got increased. Because of higher upset pressure, more heat was generated and also by slow cooling finer grains were formed. It would increase the H and TS of the plasticized zone (PZ) than in the plastically deformed zone (PDZ).

When the upsetting time was more, plastic stage material was formed as flashes and less plastic stage material was retained and more refined or fine grains were produced in the weld zone. Sathiya et al.[23] found out the influence of FW parameters on metallurgical and mechanical characteristics of ferritic stainless steel joints. Hardness was higher in the plasticized zone than in the PDZ and UZ zones. The finer grain size at the PZ was attributed to higher hardness. Fig. 7 presents the influence of rotational speed on H and TS. It shows that rotation speed varied from 1 000 to 2 000 r/min and remaining parameters namely friction pressure, upset pressure and burn-off length were kept at 85 MPa, 170 MPa and 3.5 mm, respectively. Özdemir et al.[24] stated that the ultimate tensile strength and yield strength increased with increasing rotational speed. Yilmaz et al.[25] investigated the width of the weld and weld region varying with increasing rotational speed. In FPDZ and DZ region more microstructural changes took place. In short period, high rotational speed could lead to increased temperature at the boundary. Although this condition caused reduced cooling rates and larger heat affected zone (HAZ), high rotational speed led to narrower FPDZ due to a greater volume of viscous material transferred out at the interface. The middle area of the weld was dynamically recrystallized, resulting in grain refinement which was caused due to the plastic deformation when the joint pairs were brought together with applied pressure. Thus, by increasing the

rotational speed, the weld interface region created higher temperature, due to rubbing action of the samples. The mechanical characteristic of the welded joint increased with increasing rotational speed, which caused the introduction of a higher interface temperature and repulsion of the brittle intermediate phase to outside from the interface[26,27]. Due to the formation of grain refinement, there was an increase in the H and TS of the friction welded joint. Fig. 8 presents the variation of burn-off length on hardness and tensile strength. It showed that an increase in burn-off length linearly decreased the hardness of the friction welded joint to a small extent. Increase in burn-off length dimensions increased the tensile strength of the welded joint.

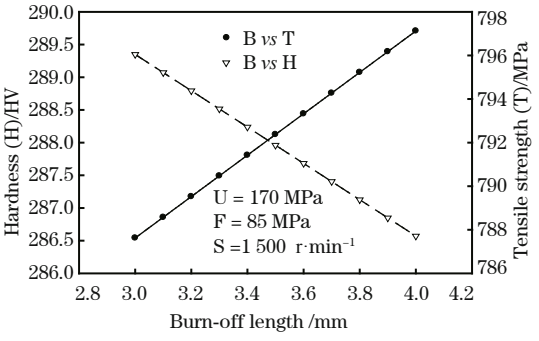

Fig. 8 Effect of burn-off length on hardness and tensile strength

6 Conclusions

(1) The plots generated from the mathematical models provided a good way for visualizing the direct and interaction effects of process parameters on the responses.

(2) The plots indicated that U, F and S were the strong determinant in changing H and TS of the friction welded joint. Hardness was found to be increasing with increasing friction force. In the case of upset force and speed being increased, hardness and tensile strength increased.

(3) The friction force was the significant parameter in changing tensile strength and hardness followed by upset force and speed rotation. Burn-off length had a negative effect on tensile strength. While burn-off length increased, the tensile strength decreased.

(4) Multi-objective optimization, carried out with the RSM model using GA approach, generated a set of Pareto optimal points. Pareto front points could aid the process operator to fix the input control variables.

(5) The selection of a point from the Pareto front would always be a trade-off between the hardness and tensile strength of the weld depending on the application.

References:

[1] Z. L. Jiang, X. Y. Chen, H. Huang, X. Y. Liu, Mater. Sci. Eng. A 363 (2003) 263-267.

[2] T. H. Chen, K. L. Cheng, J. R. Yang, Mater. Sci. Eng. A 338 (2002) 259-266.

[3] Y. H. Park, Z. H. Lee, Mater. Sci. Eng. A 297 (2001) 78-84.

[4] M. Guttmann, in: J. Charles, S. Bernhardsson (Eds.), Duplex Stainless Steel'91, Vol. 1, Les Editions de Physique, Beaune, France, 1991, pp. 79-92.

[5] J. Charles, in: J. Charles, S. Bernhardsson (Eds.), Duplex Stainless Steel'91, Vol. 1, Les Editions de Physique, Beaune, France, 1991, pp. 3-48.

[6] J. O. Nilsson, Mater. Sci. Technol. 8 (1992) 685-700.

[7] J. O. Nilsson, P. Liu, Mater. Sci. Technol. 7 (1991) 853-862.

[8] M. Nyström, B. Karlsson, ISIJ Int. 31 (1991) 738-745.

[9] J. M. Vitek, S. David, D. Alexander, J. Keiserand, R. Nanstad, Acta Metall. Mater. 39 (1991) 503-516.

[10] S. B. Dunkerton, Weld J. 65 (1986) 193-201.

[11] D. Kalyanmoy, Optimizations for Engineering Design - Algorithm and Examples, Prentice Hall of India, New Delhi, 1996.

[12] A. Khuri, J. Cornell, Response Surfaces, Design and Analysis, Marcel Dekker, New York, 1996.

[13] R. Paventhan, P. R. Lakshminarayanan, V. Balasubramanian, J. Iron Steel Res. Int. 19 (2012) No.1, 66-71.

[14] Z. Ahmet, Sahina, S. Bekir, Yibas, A. Nickel, J. Mater. Process. Technol. 82 (1998) 127-136.

[15] P. Sathiya, S. Aravindan, H. A. Noorul, K. Paneerselvama, J. Mater. Process. Technol. 209 (2009) 2576-2584.

[16] D. Ananthapadmanaban, R. V. Seshagiri, A. Nikhil, R. K. Prasad, Mater. Des. 30 (2009) 2642-2646.

[17] M. Sahin, Mater. Des. 28 (2007) 2244-2250.

[18] V. Gunaraj, N. Murugan, J. Mater. Process. Technol. 88 (1999) 266-275.

[19] Design Expert Software Version 6.0 User's Guide, 2007.

[20] R. H. Myers, D. C. Montgomery, Response Surface Methodology, Process and Product Optimization Using Designed Experiments, Wiley, New York, 1995.

[21] D. Kalyanmoy, Multi-objective Optimization Using Evolutionary Algorithms, John Wiley & Sons, Ltd., Chichester, England, 2001.

[22] S. Fukumoto, H. Tsubakino, M. Aritoshi, T. Tomita, K. Okita, Mater. Sci. Technol. 18 (2002) 219-225.

[23] P. Sathiya, S. Aravindan, H. A. Noorul, Int. J. Adv. Manuf. Technol. 31 (2007) 1076-1082.

[24] N. Özdemir, F. Sarsılmaz, A. Hascalık, Mater. Des. 28 (2007) 301-307.

[25] M. Yilmaz, M. Col, M. Acet, Mater. Charact. 49 (2002) 421-429.

[26] W. B. Lee, K. S. Bang, S. B. Jung, J. Alloys Comp. 390 (2005) 212-219.

[27] A. A. M da Silva, A. Meyer, F. Jorge, D. Santos, C. E. F. Kwietniewski, T. R. Strohaecker, Comp. Sci. Technol. 64 (2004) 1495-1501.